Inorganic Chemistry

Article

pubs.acs.org/IC

The Synthesis of a Corrole Analogue of Aquacobalamin (Vitamin B_{12a}) and Its Ligand Substitution Reactions

Caitlin F. Zipp,[†] Joseph P. Michael,[†] Manuel A. Fernandes,[†] Sadhna Mathura,[†] Christopher B. Perry,[†] Isabelle Navizet,[†] Penny P. Govender,[‡] and Helder M. Marques*[,†]

[†]Molecular Sciences Institute, School of Chemistry, University of the Witwatersrand, P.O. Wits, Johannesburg, 2050 South Africa

[‡]Department of Applied Chemistry, University of Johannesburg, P.O. Box 17011, Doornfontein, Johannesburg, 2028 South Africa

Supporting Information

ABSTRACT: The synthesis of a Co(III) corrole, [10-(2-[[4-(1*H*-imidazol-1-ylmethyl)benzoyl]amino]phenyl)-5,15-diphenylcorrolato]cobalt(III), DPTC-Co, bearing a tail motif terminating in an imidazole ligand that coordinates Co(III), is described. The corrole therefore places Co(III) in a similar environment to that in aquacobalamin (vitamin B_{12a}, H_2OCbl^+) but with a different equatorial ligand. In coordinating solvents, DPTC-Co is a mixture of five- and six-coordinate species, with a solvent molecule occupying the axial coordination site trans to the proximal imidazole ligand. In an 80:20 MeOH/H_2O solution, allowed to age for about 1 h, the predominant species is the six-coordinate aqua species [H_2O−DPTC-Co]. It is monomeric at least up to concentrations of 60 μM. The coordinated H_2O has a pK_a = 9.76(6). Under the same conditions H_2OCbl^+ has a pK_a = 7.40(2). Equilibrium constants for the substitution of coordinated H_2O by exogenous ligands are reported as log K values for neutral N-, P-, and S-donor ligands, and CN^-, NO_2^-, N_3^-, SCN^-, I^-, and Cys in 80:20 MeOH/H_2O solution at low ionic strength. The log K values for [H_2O−DPTC-Co] correlate reasonably well with those for H_2OCbl^+; therefore, Co(III) displays a similar behavior toward these ligands irrespective of whether the equatorial ligand is a corrole or a corrin. Pyridine is an exception; it is poorly coordinated by H_2OCbl^+ because of the sterically hindered coordination site of the corrin. With few exceptions, [H_2O−DPTC-Co] has a higher affinity for neutral ligands than H_2OCbl^+, but the converse is true for anionic ligands. Density functional theory (DFT) models (BP86/TZVP) show that the Co−ligand bonds tend to be longer in corrin than in corrole complexes, explaining the higher affinity of the latter for neutral ligands. It is argued that the residual charge at the metal center (+2 in corrin, 0 in corrole) increases the affinity of H_2OCbl^+ for anionic ligands through an electrostatic attraction. The topological properties of the electron density in the DFT-modeled compounds are used to explore the nature of the bonding between the metal and the ligands.

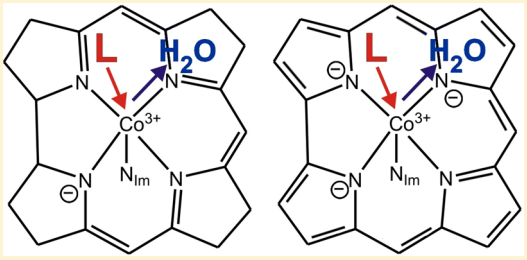

1. INTRODUCTION

Co(III) is inert in many of its complexes. For example, NMR methods show that the residence time of H_2O in $Co(III)_{aq}$ is of the order of 10^5 s,[1] compared to ca. 10^{-8} s in $Co(II)_{aq}$[2] and 10^{-5} s in $Fe(III)_{aq}$.[3] However, Co(III) is surprisingly labile in the cobalt−corrins (derivatives of vitamin B_{12}) in which the equatorial ligand is a corrin (for example, references 4−8, see Figure 1). On the basis of somewhat limited data, the approximate lability ratio of the metal ion toward substitution in corrin, porphyrin, cobaloxime, and tetraammine systems, where the equatorial ligand is a N_4 donor system (eq 1, where the entering ligand X replaces L trans to Y), is estimated to be 10^9:10^6:10^4:1.[9,10]

$$[Y - Co^{3+}(N_4) - L] + X \rightarrow [Y - Co^{3+}(N_4) - X] + L \quad (1)$$

We have been interested for some time in exploring how the equatorial ligand in the cobalt−corrins controls and modifies the properties of Co(III). Toward this end we have reported structural,[9,11,12] spectroscopic,[12,13] and density functional theory (DFT) investigations[14,15] into cobalt−corrins in which the equatorial corrin ligand has been modified, as well as the thermodynamics and kinetics of their ligand substitution reactions.[10,16−19]

When the ambidentate nucleophiles $SeCN^-$, NO_2^-, and $S_2O_3^{2-}$ replace H_2O in aquacobalamin H_2OCbl^+ (see Figure 1), they bind through the softer of the two donor atoms;[11] SCN^- is N-bound in the solid state,[11,20] but there is NMR evidence that it exists as an approximately equal mixture of the S- and N- bound species in solution.[11] The preference for the softer donor atom of the ligand suggests that Co(III) in the cobalamins is relatively soft. However, the kinetically favored product in some cases is the harder of two donor atoms of an ambident nucleophile: H_2OCbl^+ reacts initially through N of SCN^- and O of OCN^- before equilibrating to a mixture of S- and N-bound SCN^- and N-bound OCN^-.[16]

There is ample spectroscopic evidence that the positions of the principal $\pi \rightarrow \pi^*$ transitions of the corrin depend on the donor power of the axial ligand.[11,13,21,22] When the H atom at the C10 position of the corrin (Z in Figure 1) is replaced by Cl

Received: January 13, 2014
Published: April 10, 2014

   dx.doi.org/10.1021/ic5000793 | Inorg. Chem. 2014, 53, 4418−4429

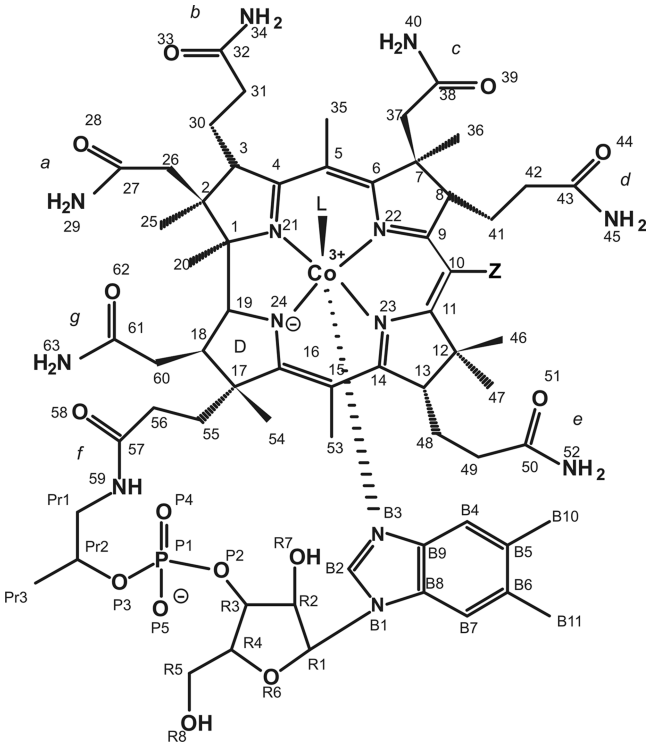

Figure 1. The standard view and numbering of the cobalamins. The axial ligand L is on the upper or β face of the corrin. In vitamin B_{12} itself (cyanocobalamin, CNCbl) Z = H, L = CN^-. Aquacobalamin (H_2OCbl^+) has Z = H, L = H_2O. The trans ligand is the base 5,6-dimethylbenzimidazole (dbzm). In cobyrinic acid, all side chain are hydrolyzed to carboxylic acids; the cobesters are esters (usually methyl esters) of cobyrinic acid.

in [L−(Co^{3+}Cbl)], L = H_2O, CN^-, Me^-, the C10−Cl bond length depends on the polarizability of L.[9] The replacement of the C10 H in H_2OCbl^+ by NO deactivates the axial coordination site toward ligand substitution.[17] Its replacement by Cl perturbs both the thermodynamics and kinetics of the substitution of axial H_2O.[10]

This accumulated evidence indicates that there is electronic communication between the axial coordination site and the equatorial ligand such that the structure of the latter can control and modify the chemistry of the former, and that Co(III) in the cobalamins is relatively soft. We have suggested[9,10,18,23] that the electron-rich equatorial corrin ligand transfers electron density to Co(III), confers on it some labile Co(II) character, and that this is the origin of the unusual kinetic lability of Co(III) in the cobalt−corrins.

We recently reported on the characterization of a dicyano stable yellow derivative of cobyrinic acid heptamethyl ester, (5*R*,6*R*)-Coα,Coβ-dicyano-5,6-dihydro-5-hydroxy-heptamethylcob(III)yrinate-*c*,6-lactone (DCSYCbs), in which the C5 carbon is oxidized such that the 13 atom, 14 π-e^- delocalized system of corrins is interrupted, giving a triazamethine system with four conjugated double bonds between N22 and N24 and an isolated double bond between N21 and C4 (see Figure 1 for numbering).[12] On the basis of ^{59}Co NMR data and the stretching frequency υ_{CN} of axially coordinated CN^-, we showed that Co(III) interacts less strongly with the equatorial ligand than in dicyano cobyrinic acid heptamethyl ester (DCCbs) itself. DFT calculations confirmed there is greater overlap between the corrin and the metal orbitals in DCCbs compared to DCSYCbs, which gives the metal in the former a softer and more covalent character.[12] The determination of equilibrium constants (log *K*) for substitution of axially coordinated H_2O in the aquacyano derivatives of these complexes, ACCbs and ACSYCbs, in which one of the cyanide ligands is replaced by H_2O by a number of anionic ligands, showed not only that the softer metal in ACCbs has a preference for softer ligands but also that the harder metal in ACSYCbs prefers the harder ligands, while the kinetics of the substitution of H_2O by CN^- demonstrated that ACCbs is more labile than ACSYCbs.[18] Log *K* values for the reaction of these compounds with neutral N-donor ligands showed that the harder Co(III) in ACSYCbs prefers aliphatic amines with a harder N donor, while the softer Co(III) in ACCbs prefers the softer N donors of aromatic amines.[19] We now take our approach of modifying the electronic structure of the equatorial ligand in the cobalt−corrins a step further by preparing a tailed corrole, culminating in an imidazole ligand, which places Co(III) in a similar coordination environment as in H_2OCbl^+ but with a corrole rather than a corrin as the equatorial ligand.

Corroles are aromatic tetrapyrrole macrocycles containing, like corrins, a direct C1−C19 pyrrole−pyrrole bridge,[21] resulting in a macrocyclic cavity topologically similar to that of corrins;[22] however, with an aromatic 18 π-electron system, they are more electron-rich.[24] Corroles are stronger acids than corrins because of the presence of three pyrrole-like and one imine-like nitrogen donors; on coordination of metal ions, corroles form trianions, whereas corrins form monoanions. Corroles are therefore capable of binding metal ions in both high and low oxidation states.[24,25]

There are a number of routes to the synthesis of corroles. The independent announcement by two groups of a facile one-pot synthesis[26,27] in 1999 led to a significant increase in the number of reports on corroles (Scheme 1, (i)). In this approach, the first step is an acid-catalyzed electrophilic substitution reaction between pyrrole and benzaldehyde derivatives, which produces polymers of various lengths with alternating pyrrole and aldehyde subunits. The second step involves use of an oxidant such as 2,3-dichloro-5,6-dicyano-1,4-benzoquinone (DDQ) or tetrachloro-1,4-benzoquinone (*p*-chloranil) in, for example, chloroform or dichloromethane, to effect an oxidative ring closure of the polymers (pyrrole−pyrrole coupling) and subsequent aromatization to yield a variety of macrocycles based on the length and identity of the polymer chain produced in the first step.[28] The desired polymer for corrole synthesis is a bilane or tetrapyrrane formed by the condensation of four pyrrole and three aldehyde subunits.[28] This approach yields A_3 corroles (A is the substituent at the 5, 10, and 15 positions) in low yields (5−15%).[26,27,29,30]

A novel method for the synthesis of mesosubstituted corroles was introduced by Koszarna and Gryko.[28] The reaction occurs in water/methanol in the presence of 0.1 equiv of HCl and exploits the difference in solubility of the starting materials and the bilane product; whereas the starting aldehyde and pyrrole, and the dipyrromethane intermediate, are soluble, the bilane tends to precipitate, effectively halting the reaction at the this stage. The isolated bilane is then oxidized to the corrole macrocycle. This procedure reduces the formation of porphyrins and other products. The use of *p*-chloranil rather than DDQ tends to increase corrole yields (typically between 13% and 56%).

A stepwise approach to a corrole usually begins with the synthesis of a dipyrromethane[28,31,32] from pyrrole and an aldehyde in the presence of a catalytic amount of acid, often trifluoroacetic acid (TFA).[33] The synthesis requires a large excess of pyrrole (typically 40:1 pyrrole/aldehyde), short reaction times,

dx.doi.org/10.1021/ic5000793 | *Inorg. Chem.* 2014, 53, 4418−4429

Scheme 1. Three Synthetic Routes to Corroles[a]

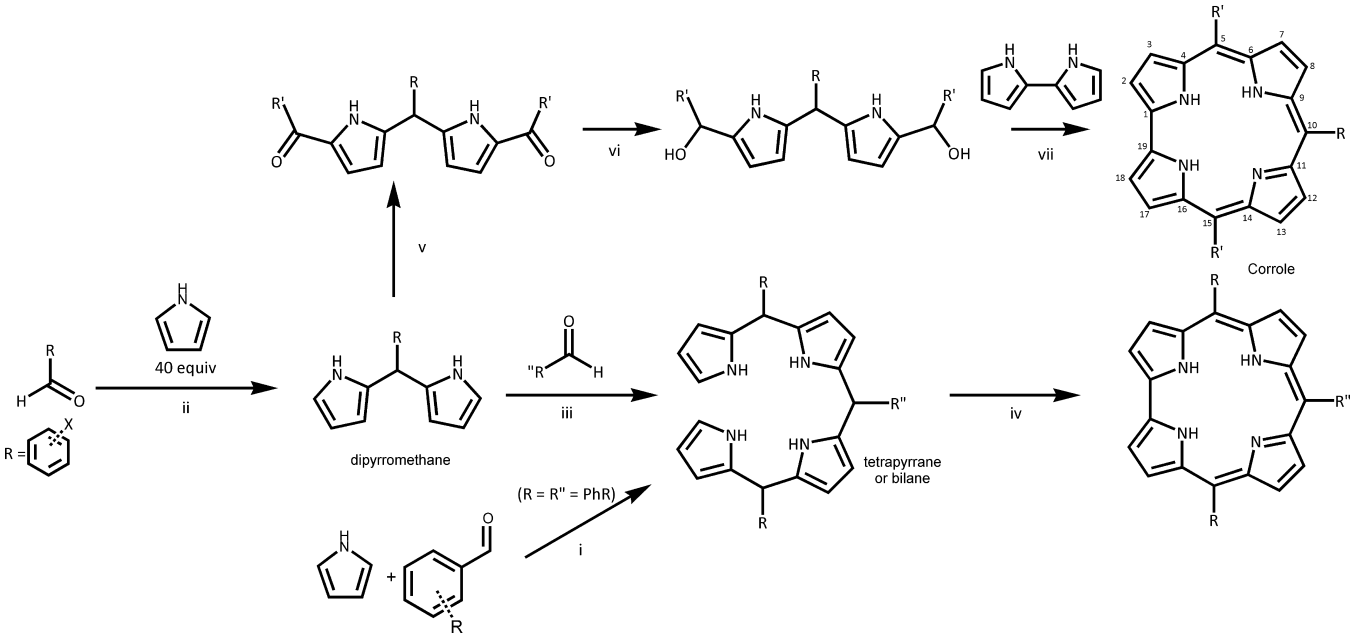

[a](i) Acid-catalyzed reaction between pyrrole and a benzaldehyde produces inter alia a bilane. Conducting the reaction in a water/methanol solvent system causes precipitation of the bilane, halting the condensation reaction at this stage. (ii) There is greater control over the synthesis of the bilane by proceeding through dipyrromethane intermediate (cat. TFA, 15 min, large excess of pyrrole). (iii) CH_3OH/H_2O 1:1, cat. HCl. (iv) *p*-Chloranil (1 equiv) (v) EtMgBr (5 equiv), R′COCl (2.5 equiv). (vi) $NaBH_4$ (50 equiv), THF/CH_3OH 3:1 or $NaBH_4$ (20 equiv), THF/CH_3OH 10:1 (anhydrous). (vii) NH_4Cl (2.5 equiv), BF_3Et_2O (0.2 equiv), CH_3CN.

and low temperature (typically 15 min, room temperature) to minimize the formation of oligomers or pyrrole polymerization. Yields are usually better than 50%. Dipyrromethane units can then be condensed with an aldehyde under acidic conditions to form a bilane. Alternatively, the corrole macrocycle is constructed from the acylation and subsequent reduction of dipyrromethane to form a dicarbinol, which is then coupled with 2,2′-bipyrrole in a [2 + 2] condensation to yield a corrole,[32,34] with decreased chance of porphyrin formation. Yields of corrole are typically up to 12%. There are several routes to the synthesis of 2,2′-bipyrrole from pyrrole.[35,36] Metalation of the corrole is usually effected by refluxing in an appropriate solvent such as methanol with a metal acetate, chloride, or carbonyl.[37]

There are relatively few studies on the ligand-substitution reactions of corroles, and to our knowledge there is only one example of a substitution reaction that has been studied in aqueous solution, namely, the binding of human serum albumin (HSA) to the gallium and manganese complexes of the water-soluble 2,17-bis-sulfonato-5,10,15(trispentafluorophenyl)-corrole.[38] Both the free base and metalated corroles bind HSA very strongly, such that the equilibrium constants for these reactions could not be determined by ultraviolet−visible (UV−vis) spectrophotometric titrations. A brief review of the available equilibrium constants is given in Section S2.1 of the Supporting Information.

To realistically mimic the coordination environment of Co(III) in H_2OCbl^+, the corrole model should (i) be soluble in water or mixed solvents with a significant amount of water, (ii) contain an aromatic N-donor as one of the axial ligands, and (iii) have H_2O as the other axial ligand. The design, synthesis, characterization, and solution behavior of such a corrole is described in this Paper. We also report equilibrium constants (log *K* values) for the substitution of coordinated H_2O by a variety of ligands and compare the results to those obtained with H_2OCbl^+ under the same conditions to assess the effect of the equatorial ligand on the coordination chemistry of Co(III).

2. RESULTS

2.1. Synthesis of a Tailed Corrole Mimic of Aquacobalamin. We explored various routes to simple corroles[39] and in our experience found Gryko's method[28] to be the most generally successful. We then set out to design a corrole bearing a "tail" substituent such that the terminus of the tail terminated in an imidazole-type ligand for Co(III), so as to have similar electronic properties to the 5,6-dimethylbenzimidazole (dmbzm) proximal ligand of H_2OCbl^+. We employed molecular mechanics methods (see Experimental Section, Table S3.1 and Figure S2 of the Supporting Information) to investigate the probable relative stability of a number of model complexes. A variety of systems with the tail extending from a C10 phenyl substituent and culminating in an aromatic N-donor were evaluated (a few examples are given in Figure S3 of the Supporting Information). Systems were evaluated based on the value of the Zindo single-point energy of the molecular mechanics energy-minimized structure, the tilt angle of the N-donor base to the corrole plane, and the requirement that the metalated corrole ring remain relatively planar, as found in the crystal structures of a number of Co(III) corroles.

The system chosen consisted of an amide and a phenyl ring (in a meta arrangement) between the meso phenyl and a terminal imidazole (Figure 2). Molecular modeling showed this system to have a relatively low energy with all structural metrics within the expected values. There was little distortion of the plane of the corrole macrocycle, and the cobalt-imidazole bond was nearly perpendicular to the mean plane of the macrocycle. The tail was less flexible than in aliphatic-based systems (Supporting Information, Figure S3) but less rigid than the

dx.doi.org/10.1021/ic5000793 | *Inorg. Chem.* 2014, 53, 4418−4429

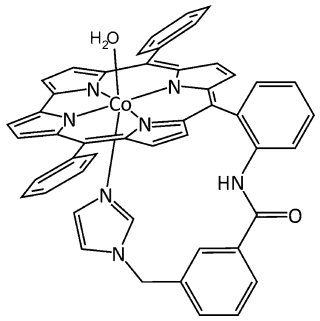

Figure 2. The basic scaffold of the chosen Co(III) corrole model for H_2OCbl^+, [10-(2-[[4-(1*H*-imidazol-1-ylmethyl)benzoyl]amino]-phenyl)-5,15-diphenylcorrolato]-cobalt(III), abbreviated as diphenyl-tailed corrole Co(III), DPTC-Co. In an 80:20 MeOH/H_2O solution, the axial coordination site is occupied by a solvent molecule (see text), and the compound is referred to as [H_2O−DPTC-Co]. Future elaboration of the two phenyl substituents with water-solubilizing groups is envisaged.

anthracene systems. This suggested that the tail would be able to rotate in solution and move into a position favorable for coordination to cobalt. Moreover, there is literature precedence for this substituent in both porphyrin[40−45] (or bearing substituents on the imidazole moiety[42,46−48]) and corrole[49] chemistry.

As the yields of corrole are usually quite low, our approach entailed the preparation of intermediates bearing the elements of the target molecule before cyclization to produce the final corrole. Therefore, an aldehyde bearing the tail motif and a dipyrromethane bearing a phenyl were prepared.

The initial idea was to prepare an imidazole acid chloride by a route described by Collman[50] (Supporting Information, Scheme S1, Section S2.2); condensation with 2-aminobenzyl alcohol and oxidation should have afforded the required tail-bearing aldehyde. As described in the Supporting Information, we were unable to prepare the acid chloride.

This difficulty was overcome by using 3-(chloromethyl)-benzoyl chloride as starting material (Scheme 2). It was first coupled to 2-aminobenzyl alcohol in dichloromethane in the presence of triethylamine in 57% yield after 2 h reaction; diffraction-quality crystals of 3-(chloromethyl)-*N*-[2-(hydroxymethyl)-phenyl]benzamide were obtained, and the molecular structure was determined by X-ray diffraction (XRD) methods (Supporting Information, Section S2.4, CCDC deposition #980627). If the reaction was allowed to proceed for more than 3 h, 2-[3-(chloromethyl)benzamido]benzyl 3-(chloromethyl)benzoate was produced instead. This too crystallized and was characterized by XRD (Supporting Information, Section S2.4, CCDC deposition #980628).

Imidazole was coupled to 3-(chloromethyl)-*N*-[2-(hydroxymethyl)phenyl]benzamide in dimethylformamide (DMF), based on Berto's synthesis,[44] to yield the alcohol *N*-[2-(hydroxymethyl)phenyl]-3-(1*H*-imidazol-1-ylmethyl)-benzamide. The use of ammonia solution rather than triethylamine to basify the work-up solution produced the alcohol in good yield and high purity. Removal of all traces of DMF was essential for the oxidation of the alcohol to the aldehyde, *N*-(2-formylphenyl)-3-(1*H*-imidazol-1-ylmethyl)benzamide, using manganese dioxide in chloroform over a 20 h period. Both the alcohol and the aldehyde were found to be crystalline and polymorphic solids; we have reported their XRD structures.[51]

This aldehyde and 2,2-(phenylmethylene)bis(1*H*-pyrrole) were used in Gryko's methanol/water corrole synthesis[28] to produce the corrole 10-(2-[[4-(1*H*-imidazol-1-ylmethyl)-benzoyl]amino]phenyl)-5,15-diphenylcorrole, referred to here as diphenyl tailed corrole (DPTC), a very dark green/purple solid that appears to be microcrystalline but did not yield diffraction-quality crystals, despite many crystallization attempts. The UV−vis spectrum of a 0.6 mM solution in hexane shows a split Soret band at 414.5 nm (ε = 3.58 × 10^3 M^{-1} cm^{-1}) and 435 nm and two bands in the visible region (579, 610 nm). The molecular ion peak was observed at m/z = 726 ([M + H]$^+$). The NH amide signal was observed at 9.04 ppm in the ^{1}H NMR spectrum, and the amide carbonyl signal was seen at 163.61 ppm in the ^{13}C NMR spectrum. Signals from the methylene group were present in both the ^{1}H and ^{13}C NMR spectra at 3.09 and 21.03 ppm, respectively. The typical

Scheme 2. Synthesis of the Tailed Aldehyde from 3-(Chloromethyl)benzoyl Chloride[a]

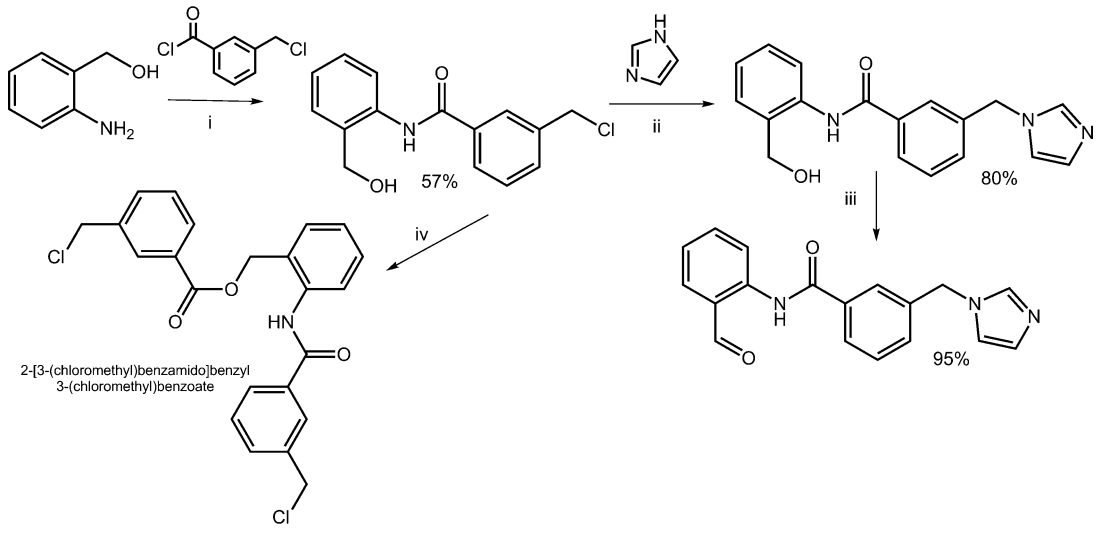

[a](i) Dry CH_2Cl_2, triethylamine, 0°C, 10 min, then room temperature, 2 h; (ii) DMF, 2 h; (iii) MnO_2, $CHCl_3$, 20 h; (iv) as in (ii) but with reaction time >3 h.

dx.doi.org/10.1021/ic5000793 | *Inorg. Chem.* 2014, 53, 4418−4429

corrole NMR signals of the β protons were present at 8.85, 8.83, 8.46, and 8.40 ppm.

Refluxing DPTC in methanol with excess cobaltous acetate and sodium acetate for 2 h produced the Co(III) corrole, [10-(2-[[4-(1*H*-imidazol-1-ylmethyl)benzoyl]amino]phenyl)-5,15-diphenylcorrolato]cobalt(III), DPTC-Co (m/z = 782.4 ($[M + H]^+$)). Metalation resulted in a general upfield shift of the ^{1}H NMR signals as a result of the shielding effect of low spin Co(III);[39] the β protons shifted from 8.85, 8.83, 8.46, and 8.40 ppm in the metal-free corrole to 8.80, 8.40 (integrating for four β protons), and 8.19 ppm in the metalated species.

2.2. The Solution Chemistry of DPTC-Co. *2.2.1. UV−Vis Spectra.* The UV−vis spectrum of DPTC-Co depends on the nature of the solvent. Representative spectra in dichloromethane, in acetonitrile, and in aqueous methanol are shown in Figure 3. The spectra in other solvents are given in Figure S4 of the Supporting Information.

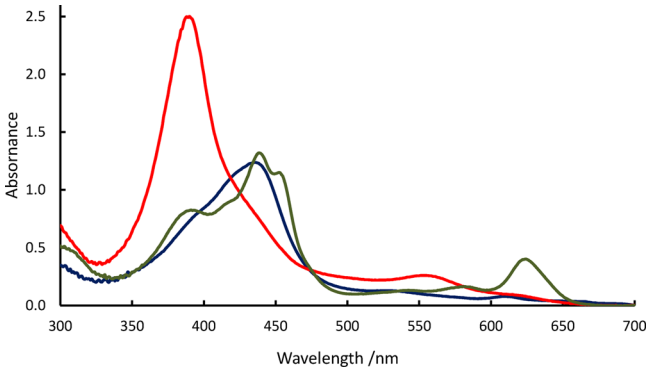

Figure 3. The UV−vis spectra of ca. 50 μM DPTC-Co in dichloromethane (red), in acetonitrile (green), and in neutral 80:20 methanol/H_2O (blue) after equilibration.

The spectrum of DPTC-Co in noncoordinating solvents such as dichloromethane, hexane, and ethyl acetate has a prominent Soret band around 390 nm, with a shoulder around 425 nm, and a broad Q band around 555 nm. The intensity of the Soret band is solvent-dependent. Coordinating solvents including acetone, methanol, acetonitrile, and tetrahydrofuran (THF) cause the Soret band to split and move to around 450 nm. In many cases (Figure 3) significant absorbance at around 390 nm remains. The broad Q band around 550 nm becomes a series of bands, with the most prominent being the longest wavelength band between 600 and 650 nm (Figure 3 and Supporting Information, Figure S4). When the compound was dissolved in 80:20 methanol/water mixtures, the intensity of its Soret at 390 nm decreased and moved to 440 nm, with a half-life of approximately 10 min at 25 °C.

To rationalize these observations, time-dependent (TD) DFT calculations were carried out on a model of DPTC-Co (Figure S5 of the Supporting Information). According to this model, two higher-intensity transitions and several lower-intensity transitions constitute the Soret region (Figure S6 of the Supporting Information); there is one principal transition in the visible region which makes up the Q band, and there are multiple transitions in the UV region. (This is discussed more fully in Section S2.5 of the Supporting Information). In the case of five-coordinate DPTC-Co, the two higher-intensity transitions in the Soret region are close together (separated by 7 nm); these will clearly overlap in the experimental spectrum and present as a fairly intense band in the near-UV region. In the calculated spectrum of [H_2O−DCTC-Co] in which H_2O occupies the sixth axial coordination site, the two most intense transitions in the Soret region are red-shifted and slightly further apart (8 nm). The Q band transition is also red-shifted (Supporting Information, Figure S6). The transitions undergo a further shift to the red in $[CN−DCTC-Co]^-$; the two principal Soret transitions are now quite far apart (25 nm) and might present in the experimental spectrum as a split Soret band.

These calculations afford a rationalization of the experimental observations shown in Figure 3. The more intense, higher-energy Soret band of DPTC-Co in DCM is consistent with a five-coordinate species. In the presence of water, the Soret broadens and shifts to the red, consistent with [H_2O−DPTC-Co] being the predominant species in solution. (In dried methanol, there is a band at 386 nm and a band at 436 nm, with a shoulder at 453 nm; see Figure S7 of the Supporting Information. This suggests a mixture of five- and six-coordinate species in solution.) In acetonitrile, the intensity at 390 nm and the split Soret at 442 and 455 nm are also indicative of a mixture of five- and six-coordinate species in solution. We shall use the nomenclature DPTC-Co to refer to the cobalt corrin in the solid state or in solvents where it exists either as a five-coordinate species or as a mixture of five- and six-coordinate species. In 80:20 MeOH/aqueous buffer solutions that have been allowed to equilibrate (see above), the predominant species is six-coordinate, and we shall refer to it as [H_2O−DPTC-Co].

2.2.2. Behavior in Aqueous Methanol Solution. The UV−vis spectrum of [H_2O−DPTC-Co] in 80:20 MeOH/H_2O changes with pH, as shown in Figure 4. This is attributed to

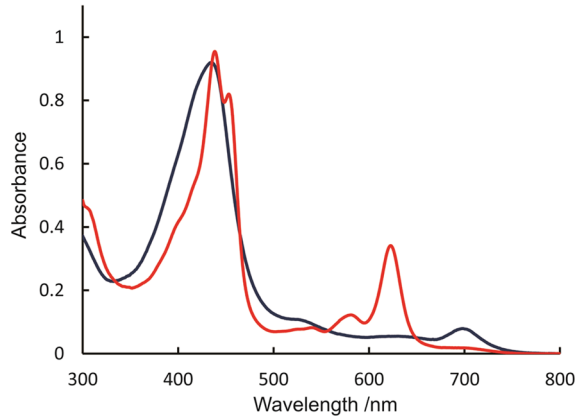

Figure 4. The dependence of the UV−vis spectrum of [H_2O−DPTC-Co] on pH in 80:20 MeOH/H_2O; pH 6.9 (blue) and pH 10.5 (red).

ionization of coordinated H_2O to form $[OH−DPTC-Co]^-$. The absorbance at the Soret maximum and the Q-band maximum at pH 9.5 were determined as a function of [H_2O−DPTC-Co] up to concentrations of 60 μM; Beer's law is strictly obeyed, which is a strong indication[52−55] that the species is monomeric in solution at least up until these concentrations.

The pK_a for the ionization of coordinated H_2O in [H_2O−DPTC-Co] was determined by titrating between pH 6.9 and 11.7 in an 80:20 MeOH/buffer solution, where the buffer consisted of 1 mM each of 3-morpholinopropane-1-sulfonic acid (MOPS), 2-amino-2-hydroxymethylpropane-1,3-diol (TRIS), and 2-(cyclohexylamino)ethanesulfonic acid (CHES). The ionic strength (μ) of the solution was very low, on average 0.8 mM across the pH range studied. The spectroscopic

dx.doi.org/10.1021/ic5000793 | Inorg. Chem. 2014, 53, 4418−4429

changes (Figure S8 of the Supporting Information) are consistent with a single $pK_a = 9.76 \pm 0.06$.

The pK_a of H_2O in H_2OCbl^+ has been reported by several workers,[5,6,9,56−62] with values varying between 7.5[61] and 8.1.[6] This variability is probably because of differences in ionic strength and, in some cases, the unfortunate use of chloride salts to adjust ionic strength (chloride will coordinate Co(III) in H_2OCbl^+, albeit weakly[16,63]). We determined the pK_a of H_2OCbl^+ using the same buffer system as for [H_2O−DPTC-Co], namely, μ = 0.8 mM in 80:20 MeOH/H_2O, as well as in aqueous solution. In aqueous and aqueous methanol solutions, we found pK_a = 7.462(7) and 7.40(2), respectively (Supporting Information, Figure S9).

2.3. Equilibrium Constants. While many equilibrium constants (log K) for substitution of coordinated H_2O in H_2OCbl^+ are available (for example, reference 64) these have all been determined in aqueous solution. To determine whether solution composition materially affected the results, we studied the substitution of coordinated H_2O by *N*-methylimidazole in very low ionic strength solutions with between 0 and 80% (v/v) MeOH (50 mM MOPS). The log K values, corrected for the effect of pH (eq 5, vide infra), are summarized in Table 1.

Table 1. Effect of Solvent Composition on the log K Value for Substitution of H_2O in H_2OCbl^+ by *N*-Methylimidazole (25 °C)

% MeOH (v/v)	polarity ($E_T(30)$)[65,66]	log K^a	μ (M)
0	63.1	4.32(4)	0.019
20	61.0	4.32(4)	0.021
40	59.3	4.21(5)	0.019
60	57.3	4.04(6)	0.022
80	56.3	3.99(5)	0.022

[a]Corrected for pH (eq 5).

The composition of the solvent has a small but significant effect on the values of log K. A similar effect, for the substitution of H_2O by pyridine in aquacyanocobyrinic acid, has been reported by Hamza.[67] We therefore determined all log K values for both [H_2O−DPTC-Co] and H_2OCbl^+ under the same conditions (25 °C, 80% MeOH, 20% CAPS, CHES, MOPS, or MES buffer, v/v, $\mu \approx 0.02$ M).

Figure S10 of the Supporting Information shows, as an example, the spectroscopic changes associated with the substitution of H_2O in [H_2O−DPTC-Co] by dimethylaminopyridine (DMAP), and Supporting Information, Figure S11 shows the spectroscopic changes where the incoming ligand is N_3^-.

To verify the validity of the correction for the pK_a of [H_2O−DPTC-Co] (eq 5), we determined log K values for coordination of NO_2^- at pH values above and below the pK_a value of [H_2O−DPTC-Co], which is 9.76(6)). The results are listed in Table 2. The observed log K values are clearly dependent on pH, but become pH-independent, 3.02(10), once they are corrected for the pK_a of [H_2O−DPTC-Co].

Table 2. Effect of pH on the log K Value for Substitution of H_2O in [H_2O−DPTC-Co] by NO_2^- (25 °C)

pH	log K_{obs}	log K^a
10.91	1.77(12)	2.95(12)
10.02	2.60(7)	3.05(7)
9.51	2.86(6)	3.06(6)
8.78	2.97(17)	3.01(17)

[a]Corrected for the pK_a of DPTC-Co (eq 5)

If the log K values were too large for direct spectrophotometric determination, they were determined in a competition experiment. For example, log K for binding of trimethylphosphite (TMP) by [H_2O−DPTC-Co] was determined by titrating aliquots of this ligand into a solution of the DMAP complex of the corrole. Log K(TMP) could then be determined from the previously measured value of log K(DMAP) and the observed log K from the titration since log K(obs) = log K(DMAP) + log K(TMP). The values of log K obtained are summarized in Table 3.

3. DISCUSSION

The pK_a values of coordinated H_2O in H_2OCbl^+ and DPTC-Co in the same solvent and ionic strength (80:20 MeOH/H_2O, μ = 0.8 mM), namely, 7.462(7) and 9.76(6), respectively, are indicative of the somewhat different nature of the Co−O bond in these two compounds. We have previously shown that replacing the C10 H with electron-donating Cl in H_2O(10Cl-Cbl)$^+$ decreases the pK_a of coordinated H_2O from 8.09 (aq solution, μ = 0.5 M, $NaNO_3$) to 7.65,[9] while replacing it with electron-withdrawing NO increases the pK_a to 10.71 (aq solution, μ = 2.2 M, $NaClO_4$). We used semiempirical MO calculations to rationalize this observation, showing that the Co−O bond in H_2O(10Cl-Cbl)$^+$ and H_2O(10NO-Cbl)$^+$ is more covalent and more ionic, respectively, than it is in H_2OCbl^+ itself. A more ionic Co−O bond makes the lone pair on coordinate OH^- more readily available, resulting in its protonation at a higher pH of the solution. We find a similar trend in our models of H_2OCbl^+ and [H_2O−DPTC-Co], on which we performed DFT calculations. The value of the electron density at the bond critical point ρ_b is a measure of the strength of the bond.[73−77] The ratio $|V_b|/G_b$, where V_b and G_b are the potential and kinetic energy densities at the bond critical point of a chemical bond, is useful to characterize the nature of the bond:[78] $|V_b|/G_b < 1$ is characteristic of an ionic bond, and $|V_b|/G_b > 2$ is characteristic of a covalent bond; a bond of intermediate character has $1 < |V_b|/G_b < 2$. Moreover, for a metal−ligand interaction, ρ is usually close to zero and the Laplacian at the bond critical point, $\nabla^2\rho > 0$. The Co−O bond in H_2OCbl^+ is shorter (2.107 Å), stronger (ρ_b = 0.0551 au, where 1 au of ρ_b = 6.7483 e Å^{-3}, $\nabla^2\rho$ = 0.2968 au, where 1 au of $\nabla^2\rho$ = 24.099 e Å^{-5}), and more covalent ($|V_b|/G_b$ = 1.0873) than that in [H_2O−DPTC-Co] (2.126 Å; 0.0508 au; 0.3785 au; 1.0695). Therefore, the more ionic Co−O bond in [H_2O−DPTC-Co] is associated with a higher pK_a value for coordinated H_2O.

The solvent can have a significant effect on the value of log K (Table 1). The log K values for neutral ligands tend to be higher in aqueous solution than in 80% MeOH, but the converse is usually true for anionic ligands (Table 4). Others have reported similar observations. Balt and co-workers found that in acetonitrile−water mixtures the equilibrium constants for the binding of thiocyanate to H_2OCbl^+ increased from log K = 3.03 to 4.17 as the fraction of acetonitrile increased from 0 to 80%;[79] Moreno-Esparza and co-workers reported that log K for the binding of iodide increased from 1.41 to 3.95 as the methanol fraction increased from 0 to 100%.[72] The effect is presumably a consequence of differential solvation of the entering ligand. This should manifest itself as a significant dependence of log K on the ΔS of the reaction and will require a study of the effect of temperature and solvent composition on log K; this is beyond the scope of the present work.

In Figure 5 the log K value for coordination of a ligand by [H_2O−DPTC-Co] is plotted against log K for its coordination

dx.doi.org/10.1021/ic5000793 | Inorg. Chem. 2014, 53, 4418−4429

Table 3. Stability Constants for the Coordination of Ligands by DPTC-Co and H_2OCbl^+ (80% MeOH, 25 °C, $\mu \approx 0.02$ M)

ligand	H_2OCbl^+			[H_2O–DPTC-Co]		
	pH[a]	log K	log K (aq sol)	pH[a]	log K	ligand stoichiometry[b]
Neutral Ligands						
ethanolamine	8.12	3.60(5)		9.50	5.15(2)	1.19(2)
pyridine	7.20	0.48(4)	1.23[10]	9.16	4.11(2)	1.04(1)
dimethylaminopyridine (DMAP)	9.10	3.99(2)		9.51	5.32(2)	1.10(1)
N-methylimidazole	7.07	3.99(5)	4.44[68]	9.46	5.41(4)	
thiophene	9.14	1.0(2)		9.52	1.09(4)	
thiourea	7.08	1.76(2)	1.1[69]	9.47	2.1(1)	
trimethylphosphite (TMP)	7.07	4.77(7)	5.0[70]	9.44	11.8(1)[c]	
trimethylphosphite (TMP)				9.50	10.4(1)[d]	
Anionic Ligands						
cysteine	6.01	6.5(1)	6.0[71]	9.87	5.7(2)	1.07(4)
cyanide	7.09	12.53(7)[e]	>12[60]	9.59	13.1(7)[f]	
	7.07	11.9(5)[g]		9.51	13.2(6)[h]	
nitrite	7.12	6.7(4)	5.34[10]	8.78	3.0(1)	0.96(2)
azide	7.11	6.35(5)	4.85[10]	9.51	2.82(2)	0.98(2)
thiocyanate	7.12	4.73(4)	3.03[10]	9.50	1.31(5)	
iodide	6.99	3.96(2)	1.4[10]	9.63	2.33(3)	

[a]The pH at which log K was determined; corrected log K values (eq 5) are reported in this table. [b]See Experimental Section. [c]Competition experiment with DMAP. [d]Competition experiment with pyridine. [e]Competition experiment with azide. [f]Competition experiment with DMAP, in cell. [g]Competition experiment with nitrite. [h]Competition experiment with DMAP, out of cell.

by H_2OCbl^+. The log K values are reasonably correlated (i.e., the general behavior of Co(III) toward the range of ligands studied is similar whether the equatorial ligand is corrin or corrole). Pyridine is an exception: it is poorly coordinated by H_2OCbl^+, and log K is anomalously low (0.48(4)); however, log K for coordination of DMAP (3.99(2)) is significantly higher. In the absence of a crystal structure, we used DFT calculations to rationalize this observation. As shown in Figure S12 of the Supporting Information, the sentinel methyl groups C54 and C46 and the methylenes C26 and C37 of the *a* and *c* acetamide side chains on the sterically crowded β face confine pyridines to the C5—C15 vector, and there is close contact between the C2 and C5 hydrogens on pyridine and C5 and C15 of the corrin, respectively. This results in a relatively long Co–N_{py} bond (2.045 Å). The presence of electron-donating NMe_2 in the para position decreases the bond length to Co(III) (2.027 Å); the corrin ring is flattened, and the nonbonded contacts become marginally longer. In DMP, therefore, the electronic influence of the para substituent overrides the steric constraints of the crowded β face of the corrin.

The ligands fall into two classes. [H_2O–DPTC-Co] has a higher affinity for neutral ligands than H_2OCbl^+, but the converse is true for anionic ligands. CN^- is an exception, but it must be appreciated that the very large values of log K for the coordination of TMP by [H_2O–DPTC-Co] and for CN^- by both [H_2O–DPTC-Co] and H_2OCbl^+ makes it difficult to obtain accurate values (Table 4). [H_2O–DPTC-Co] is neutral, whereas H_2OCbl^+ has a +2 charge at the metal center (if it is assumed that the charge on phosphate is too remote to affect matters). This therefore suggests that an electrostatic interaction between the metal center and an incoming anionic ligand is a significant contributor to the affinity of H_2OCbl^+ compared to [H_2O–DPTC-Co] for anionic ligands. This observation is in agreement with our recent observations in a comparison in aqueous solution of the coordination chemistry of Co(III) in H_2OCbl^+ and in a Co(III) analogue in which corrin was replaced by a porphyrin;[23] we found that H_2OCbl^+, with its +2 charge at the metal center, binds anionic ligands with a greater affinity than the porphyrin analogue (the charge at the metal center of a Co(III) porphyrin is +1). Conversely, the Co(III) porphyrin tended to bind neutral ligands with a higher affinity than the Co(III) corrin.

A quantum theory of atoms in molecules (QTAIM) analysis[80] of the topological properties of the electron density at the bond critical points is a useful way of exploring the nature of the bonding in transition-metal complexes.[81−86] To explore this in these Co(III) corrole and corrin complexes we chose pyridine, imidazole, and TMP as representative neutral ligands; CN^-, NO_2^-, and CH_3S^- as representative anionic ligands; and H_2O to model the starting complexes of the ligand-substitution reactions under consideration. The data are summarized in Table 4.

As expected,[73−77] there is a strong correlation between ρ_b and the bond length between Co(III) and the axial ligands (Supporting Information, Figure S13). In the aqua complex of both corrole and corrin, the bond to axial H_2O is long and weak, which is clearly the reason why it is readily displaced by other ligands. There is a normal trans influence in both systems; that is, there is an inverse correlation between the length of the Co–L bond length and the length of the Co–N_{ax} band to the proximal imidazole ligand (Supporting Information, Figure S14), although the two ligands with S and P donors do not follow this trend.

With the exception of H_2O, the bond lengths between Co(III) and L are longer in the corrin complexes than they are in the corrole complexes (i.e., $\Delta r_{corrin-corrole} > 0$, and on average $\rho_{L-Co\ (corrin)} < \rho_{L-Co(corrole)}$); however, the difference is greater for the neutral ligands ($\Delta r_{corrin-corrole}$ = 0.038(15) Å) than it is for the anionic ligands ($\Delta r_{corrin-corrole}$ = 0.013(7) Å), see Table S2 of the Supporting Information. This is precisely what we found in our recent comparison of the coordination chemistry of Co(III) corrins and porphyrins[23] and suggests that the electrostatic attraction between an anionic ligand and the residual +2 charge at the metal center of a corrin is one of the reasons why the stability of the L–Co–Cbl^+ when L is an anion is increased relative to that of the corrole complex.

dx.doi.org/10.1021/ic5000793 | Inorg. Chem. 2014, 53, 4418−4429

Table 4. Topological Properties at the Bond Critical Points of the Axial Ligands of [L−DPTC-Co] and [L−Co^{III}(corrin)−Im] Complexes from a DFT Model (BP86/TZVP)

L	Co−L (Å)	ρ^a	$\nabla^2\rho$	$\lvert V\rvert/G$	ε	DI(Co,L)^b	Co−N$_{ax}$^{c} (Å)	ρ	$\nabla^2\rho$	$\lvert V\rvert/G$	ε	DI(Co,L)
	corrole							corrin				
H_2O	2.128	0.053 83	0.272 32	1.101 44	0.034 93	0.350	1.900	0.107 62	0.484 60	1.174 85	0.042 48	0.682
py	1.989	0.088 19	0.377 72	1.169 85	0.088 61	0.580	1.969	0.090 77	0.404 61	1.161 85	0.075 61	0.569
imidazole	1.961	0.090 26	0.431 50	1.132 41	0.045 46	0.530	1.967	0.0886	0.459 20	1.129 49	0.043 15	0.520
TMP	2.182	0.099 02	0.140 28	1.541 55	0.011 91	0.782	2.076	0.071 16	0.295 72	1.159 92	0.045 73	0.435
NO_2^-	1.945	0.104 08	0.402 66	1.212 50	0.108 72	0.598	2.083	0.066 27	0.328 84	1.119 94	0.079 36	0.387
CH_3S^-	2.291	0.080 82	0.099 16	1.520 44	0.051 75	0.836	2.106	0.0628	0.308 44	1.120 14	0.045 83	0.356
CN^-	1.853	0.134 62	0.319 41	1.424 71	0.002 49	0.827	2.122	0.060 15	0.300 67	1.115 40	0.043 54	0.342

^{a}All values in au; 1 au of ρ = 6.7483 e Å^{-3}; 1 au of $\nabla^2\rho$ = 24.099 e Å^{-5}. ^{b}The delocalization index, a measure of the number of electron pairs shared between Co and L. ^{c}N$_{ax}$ refers to the N donor of proximal axial imidazole ligand trans to L.

Figure 5. Correlation of log K for coordination of neutral (blue circles) and anionic (red squares) by H_2OCbl^+ and [H_2O−DPTC-Co] in 80:20 MeOH/H_2O at 25 °C. The dotted line is the equivalue line. Abbreviations: tu = thiourea; tp = thiophene; TMP = trimethylphosphite; DMAP = *N*,*N*-dimethylaminopyridine; NMeIm = *N*-methylimidazole; Py = pyridine.

The data in Table 4 show that the metal−ligand bonds in both the corrole and corrin systems are predominantly ionic (ρ close to zero, $\nabla^2\rho > 0$, and $|V|/G$ close to 1), although there is increasing covalent character (assessed by $|V|/G$ and by the delocalization index DI, a measure of the average number of electrons shared between Co and the donor atom of the ligand) as the richness of electron density on the ligand increases (H_2O < imidazole < pyridine < NO_2^- < CN^- < TMP < CH_3S^-). CN^- (corrole, corrin) and TMP (corrole) have very high log K values for coordination to Co(III), and the bond between their donor atom and the metal has considerable covalent character. Yet cysteine (modeled by CH_3S^- in our DFT calculations) also has a Co−S bond with very significant covalent character but considerably smaller log K in both systems. Thus, while there may be some dependence of log K on the metal−ligand bond, that dependence is weak (Figure S15 of the Supporting Information, r^2 = 0.32, p = 5.3%).

The ellipticity of a bond ($\varepsilon = |\lambda_1|/|\lambda_2| - 1$, where λ_1 and λ_2 are the eigenvalues of the Hessian matrix of the electron density at the bond critical point (bcp) along mutually perpendicular axes, which are themselves perpendicular to the bond path) is a function of the ratio of the rate of electron density decrease in the two directions perpendicular to the bond path at the bcp.[80] If there is significant π bonding between two atoms then $|\lambda_1| > |\lambda_2|$ and ε will be significantly greater than 0. For example, in our model of the imidazole complex of the Co(III) corrin, the C5−C6 bond, part of the delocalized system of the corrins, presents with λ_1 = −0.6720 au and λ_2 = −0.5299 au such that ε = 0.2727. By contrast, for the C7−C8 single bond, λ_1 = −0.4339 au, λ_2 = −0.4334 au, and ε = 0.0010. The values of λ_1, λ_2, and λ_3 for all Co−L bonds modeled in this work are summarized in Table S3 of the Supporting Information.

When compared to the other Co−L bonds, we find that the bond between NO_2^- and Co(III) in both the corrole and the corrin system has significant ellipticity; this is indicative of the participation of a frontier π^* orbital in the bonding with the

dx.doi.org/10.1021/ic5000793 | Inorg. Chem. 2014, 53, 4418−4429

metal. In the case of CN^-, while ε is small, this masks the relatively large values of both λ_1 and λ_2, suggesting that both frontier π^* orbitals are involved in the bonding. We found similar effects in the bonding of NO_2^- and CN^- with Co(III) in a Co(III) porphyrin.[23]

4. CONCLUSION

We report the synthesis and characterization of a Co(III) corrole that places the metal ion in a similar coordination sphere as in aquacoabalamin, H_2OCbl^+; Co(III) is coordinated in the proximal coordination site by imidazole (cf. 5,6-dimethylbenzimidazole in H_2OCbl^+) and has a weakly bound H_2O ligand in the sixth coordination site that is readily replaced by exogenous ligands. Equilibrium constants (log K) values for replacement of H_2O by a variety of neutral and anionic ligands were determined in aqueous methanol solutions under conditions where the Co(III) corrole is monomeric. We find that Co(III) behaves similarly toward ligands whether it is in a corrin or a corrole. However, based on DFT modeling, bonds between it and axial ligands are longer in a corrin than in a corrole, explaining why in general log K values for coordination of neutral ligands are larger in a Co(III) corrole than they are in a Co(III) corrin. If L is an anion, then the difference in bond lengths becomes significantly smaller, and we suggest that an electrostatic interaction between the ligand and the residual +2 charge at the metal center in the corrin enhances the affinity of Co(III) for the ligand such that log K values for coordination of anions is larger in the corrin system than it is in the corrole system. This work highlights how the nature of the equatorial ligand in Co(III) chemistry can significantly modify the chemistry of the axial coordination site of these compounds and provides an indirect answer to the otherwise surprising fact that normally inert Co(III) is used as coenzyme in biology. The influence this has on the kinetics of ligand substitution has also been investigated and will be reported elsewhere.

5. EXPERIMENTAL SECTION

Experimental details of materials and methods used in the synthesis of DPTC-Co are given in the Supporting Information (Section S2). Deionized water, purified using a Direct Q UV 3 Millipore system and further purified using a Millipore Milli-Q unit (>18 mΩ), was used throughout this study. Hydroxocobalamin was from Roussel. pH measurements were performed using a Metrohm High-precision 780 pH meter and a Metrohm Unitrode combination pH electrode. Metrohm ready-to-use buffer solutions at pH 4, 7, and 9 were used to calibrate the electrode. The pH readings in methanol/water mixtures are uncorrected. UV−vis spectra were recorded using 1.00 cm path length cells on either a Cary 1E UV−vis or a Cary 300 Bio UV−vis Spectrophotometer, fitted with a Cary Dual Cell Peltier accessory from Varian, set at 25.0 °C, or a Cary 3E UV−vis spectrophotometer, fitted with a circulating water bath maintained at 25.0 ± 0.1 °C. Spectra were recorded with a spectral bandwidth of 2 nm, signal averaging time of 0.5 s, data interval of 1.00 nm, and scan rate of 120 nm min^{-1}. Ligand-binding isotherms were fitted with standard nonlinear least-squares methods using SigmaPlot.[87]

Proton NMR data were recorded at 300.13 MHz, and carbon NMR data were recorded at 75.47 MHz on a Bruker AVANCE 300 spectrometer. Spectra of corrole macrocycles were recorded on a Bruker ULTRASHIELD 500 PLUS spectrophotometer where proton NMR data were recorded at 500.13 MHz and carbon NMR data were recorded at 125.77 MHz. All samples were dissolved in $CDCl_3$. Chemical shifts are reported on the δ scale (parts per million (ppm)) relative to the internal standard of 0.03% tetramethylsilane (^1H) and the central $CDCl_3$ line at 77.00 ppm (^{13}C). NMR spectroscopic data were processed using the MestReNova software suite of programs.[88]

Low sample concentrations (1 mg mL^{-1}) had to be used; at higher concentrations, broad signals with no multiplet resolution were observed. It is thought that this arose from aggregation of macrocycles in solution due to significant $\pi\cdots\pi$ interaction. The available solid-state structures of corroles related to DPTC show such interactions in the solid state.[39]

Determination of the Molar Absorptivity of DPTC-Co. The absence of a crystal structure of DPTC-Co required an indirect determination of the molar absorptivity ε, which was required for determining equilibrium constants (see below, eq 4), since the solid state could well include solvent molecules as found for example in all crystal structures of the cobalt−corrins. A series of cobalt standards was prepared using dicyanocobalamin, prepared by treating a solution of aquacobalamin with excess cyanide and waiting until there was no further change in the UV−vis spectrum. Using the well-established value of $\varepsilon_{367} = 3.04 \times 10^4$ M^{-1} cm^{-1},[89] the concentration of the solutions could be determined. The concentration of Co was determined by atomic absorption spectroscopy on a PG-900 atomic absorption spectrophotometer using a graphite furnace fitted with a pyrolytically coated HGA-76 graphite tube and a Photron hollow-cathode lamp single element cobalt lamp. The absorption line characteristic of Co at 240.7 nm was integrated using the AAWin software suite.[90] Nonspecific absorption of radiation was corrected for by subtracting the absorbance recorded from a deuterium lamp.[91] We obtained a linear response up to a concentration of 0.2 ppm of Co. Samples of DPTC-Co in dichloromethane were prepared from a sample of DPTC-Co dried on a high vacuum line, which was weighed and diluted to give an approximate Co concentration of 0.1 ppm. The relative standard deviation of the measurements of the samples and standards was <2%. We found that in dichloromethane $\varepsilon_{389} = 5.14 \times 10^4$ M^{-1} cm^{-1} for DPTC-Co. Values of ε in other solvents (and hence the concentration of DPTC-Co) could be determined by comparing the spectra of aliquots of a stock solution of DPTC-Co in dichloromethane and in the solvent of interest.

Equilibrium Constants. The equilibrium constants, K, for the coordination of the ligands by [H_2O−DPTC-Co] and aquacobalamin (vitamin B_{12a}, H_2OCbl^+), eq 1, where coordinated H_2O (or possibly MeOH) is displaced by the exogenous ligand L, N_{ax} is the trans N-donor ligand (imidazole in DPTC-Co and 5,6-dimethylbenzimidazole in H_2OCbl^+), N_4 represented the equatorial macrocycle corrole or corrin, and the overall charge is omitted for convenience, were determined by addition of aliquots of a stock solution of the appropriate ligand to a 20−50 μM solution of the Co(III) complex contained in a 1.00 cm path length cuvette housed in the thermostated cell block of a UV−vis spectrophotometer. The solvent was 80:20 MeOH/H_2O and 0.05 M in the appropriate buffer (CAPS, for pH > 10; CHES, for pH 8.5−10; MOPS for pH 7−8; MES for pH 6−7). Typically between 12 and 18 aliquot additions were made in each titration, and absorbance readings were corrected for dilution. For cases where log K is relatively small (log K < 4), the absorbance data at wavelength λ were fitted using nonlinear least-squares methods to a simple binding isotherm (eq 3) as objective function, with A_0, A_1, and K as the parameters to be optimized. A_0 and A_1 are the absorbance values at λ corresponding to 0 and 100% complex formation, respectively.

$$[N_{ax} - Co(N_4) - OH_2] + L \rightleftharpoons [N_{ax} - Co(N_4) - L] + H_2O \quad (2)$$

$$A_\lambda = (A_0 + KA_1[L])/(1 + K[L]) \quad (3)$$

When log K is relatively large (>4), the implicit assumption in eq 3 that $[L]_{free} \approx [L]_{total}$ is not true because a significant fraction of the added ligand will be complexed to the metal ion. In this case [L] in eq 3 has to be replaced by an explicit expression for $[L]_{free}$. It can be shown[92] that $[L]_{free}$ is given by eq 4, where only one root has physical meaning. In eq 4, $[M]_{total}$ is the total metal ion concentration.

$$[L]_{free} = \frac{-a_2 \pm \sqrt{a_2^2 - 4a_1a_3}}{2a_1}$$

$$a_1 = K;\ a_2 = 1 + K[M]_{total} - K[L]_{total};\ a_3 = -[L]_{total} \quad (4)$$

dx.doi.org/10.1021/ic5000793 | Inorg. Chem. 2014, 53, 4418−4429

It is well-established in cobalt−corrin chemistry that hydroxide in hydroxocobalamin will not be displaced by an exogenous ligand L.[5,93,94] Moreover, it is usually the case that the protonated form of a ligand (for example, imidazole) will not coordinate to a metal ion. Conditional stability constants K_{obs}, determined at some pH value, were therefore converted to pH-independent equilibrium constants K, using eq 5, where pK_{aL} refers to the acid dissociation constant of the conjugate acid of ligand L and the pK_{aM} value, to the acid dissociation constant of coordinated H_2O in DPTC-Co and H_2OCbl^+.

$$K = K_{obs}(1 + 10^{pK_{aL}-pH})(1 + 10^{pH-pK_{aM}}) \quad (5)$$

The spectroscopic changes were recorded between 300 and 800 nm; typically between 4 and 6 wavelengths where absorbance changes were largest were fitted to eq 3 or eq 4, as appropriate. A weighted average (with the weighting as the reciprocal of the relative percentage error of the fit) of the results obtained at the monitoring wavelengths was calculated.

The ligand stoichiometry associated with some titrations of [H_2O−DPTC-Co] was determined from the slope of a Hill plot, a plot of log [L] against log $((A_0 - A)/(A - A_1))$, where A is the absorbance associated with each concentration of the incoming ligand L; the other variables have been defined (vide supra).

Molecular Mechanics. The Generalized AMBER Force Field (GAFF)[95] as implemented in HyperChem 7,[96] and expanded for the cobalt−corrins,[97] was used for exploring potential Co(III) corrole models of H_2OCbl^+. The force field was augmented for modeling corroles as follows. A search of the Cambridge Structural Database[98] using ConQuest[99] for Co(III) corroles yielded 10 structures, for which eight new atom types were defined as illustrated in Figure S2 of the Supporting Information. Initial values of both lengths, bond angles, torsional angles, and the bond stretch and angle-bending force constants involving the metal ion were arrived at by analogy with the cobalt−corrins force-field values[97] and informed by the crystallographic data. Parameters for the pyrrolic and meso carbon atom were based on standard GAFF values for organic systems. These initial parameters were then used to model Co(III) triphenylcorrole. All bond lengths, angles, and torsions were measured and compared to the crystallographic data. If the parameters produced structural metrics within one standard deviation of the mean of the 10 crystallographic structures, they were accepted. Otherwise they were adjusted on a trial-and-error basis until this level of agreement was reached. The final parameters are listed in Table S1 of the Supporting Information. Geometry optimization was carried out using the Polak−Ribiére conjugate gradient algorithm with a convergence criterion of 0.05 kcal $Å^{-1}$ mol^{-1}. Single-point energy calculations on the molecular-mechanics optimized geometry were carried out using the semiempirical Zindo method.[100]

DFT and QTAIM Calculations. DFT calculations were performed on a simplified model of DPTC-Co (Figure S5 of the Supporting Information) in vacuo. The tail was truncated at the amide moiety, and imidazole was used as the proximal axial ligand. Calculations were also carried out on a simplified model of H_2OCbl^+ with all substituents on the corrin replaced by H, and the dimethylbenzimidazole base replace by imidazole. Calculations were carried out using Gaussian-09,[101] the BP86 functional,[102,103] and the TZVP basis set.[104,105] In addition, to help speed up the calculations we made use of the density-fitting approximation,[106,107] and the density-fitting TZVP basis set as well.[108,109] TD-DFT single-point excitation energies for the first 30 excited states were calculated using the hybrid density functional CAM-B3LYP[110] with TZVP basis set. The electron density at the Co−L bond critical points was analyzed using Bader's QTAIM[80] as implemented in AIMALL;[111] for this purpose, the wave function files were generated using Gaussian-09 for input into AIMALL.

■ ASSOCIATED CONTENT

Supporting Information

Dependence of equilibrium constants of coordination by Co(III) corroles on the pK_a of the entering ligand (Figure S1); new atom types defined for molecular mechanical calculations of cobalt−corroles (Figure S2); a selection of Co(III) corrole modeled by molecular mechanics methods as potential targets (Figure S3); UV−vis spectra of DPTC-Co in a variety of solvents (Figure S4); representation of the simplified model of DPTC-Co used for DFT calculations (Figure S5); CAM-B3LYP/TZVP TD-DFT spectra of five-coordinate DPTC-Co, [H_2O−DPTCCo], and [CN−DPTCCo]$^-$ (Figure S6); UV−vis spectrum of DPTC-Co in dried methanol and in 80:20 MeOH/H_2O (Figure S7); dependence of the absorbance at 621 nm of [H_2O−DPTC-Co] on pH in 80:20 MeOH/H_2O (Figure S8); dependence of the absorbance at 350 nm of H_2OCbl^+ on pH in aqueous solution and in 80:20 MeOH/H_2O (Figure S9); spectroscopic changes observed on titrating [H_2O−DPTC-Co] in 80% MeO/H_2O with dimethylaminopyridine (Figure S10) and with N_3^- (Figure S11); depiction of DFT-optimized B_{12} complexes with pyridine and dimethylaminopyridine (Figure S12); correlation in DPTC-Co and Co(III) corrin complexes between the axial bond length to the proximal imidazole ligand and the trans ligand L, and the electron density at the Co−imidazole and Co−L bond critical points (Figure S13); dependence of the trans Co−N_{ax} bond length to imidazole in DFT models of [L−DPTC-Co] and) [L−Co(corrin)−Im] on the Co−L bond length (Figure S14); correlation between $|V|/G$ at the bond critical point of the Co−ligand bond in DFT models (BP86/TZVP) of Co(III) corrole and Co(III) corrin complexes, and the experimentally determined log K values for substitution of axial H_2O (Figure S15); a brief review of the ligand-substitution reactions of Co(III) and Mn(III) corroles (Section S2.1); account of the attempted synthesis of an aldehyde bearing the tail motif (Section S2.2); detailed description of the synthesis of DPTC-Co (Section S2.3); crystallographic details of molecular structures reported in this work (Section S2.4); account of the TD-DFT calculations (Section S2.5); tables of new AMBER parameters for modeling Co(III) corroles (Table S3.1); comparison of axial bond length distances in DFT (BP86/TZVP) models of [L−Co(N_4)−N_{ax}] complexes (Table S3.2); and eigenvalues of the Hessian of the electron density at the bond critical point of Co−L bonds, and bond ellipticity, in DFT Models (BP86/TZVP) in corrole and corrin complexes (Table S3.3); 37 pages. This material is available free of charge via the Internet at http://pubs.acs.org.

■ AUTHOR INFORMATION

Corresponding Author

*E-mail: Helder.Marques@wits.ac.za. (H.M.M.)

Notes

The authors declare no competing financial interest.

■ ACKNOWLEDGMENTS

The financial assistance of the Department of Science and Technology, the National Research Foundation, Pretoria, through SARChI, the South African Research Chairs Initiative, the University of the Witwatersrand, Johannesburg, and the Andrew P. Mellon Foundation is gratefully acknowledged.

■ REFERENCES

(1) Rutenberg, A. C.; Taube, H. *J. Chem. Phys.* **1952**, *20*, 825−826.
(2) Swift, T. J.; Connick, R. E. *J. Chem. Phys.* **1962**, *37*, 307−320.
(3) Fiat, D.; Connick, R. E. *J. Am. Chem. Soc.* **1968**, *90*, 608−615.
(4) Poon, C. K. *Coord. Chem. Rev.* **1973**, *10*, 1−35.
(5) Reenstra, W. W.; Jencks, W. P. *J. Am. Chem. Soc.* **1979**, *101*, 5780−5791.
(6) Marques, H. M.; Brown, K. L.; Jacobsen, D. W. *J. Biol. Chem.* **1988**, *263*, 12378−12383.

(7) Stochel, G.; van Eldik, R.; Kunkely, H.; Vogler, A. *Inorg. Chem.* **1989**, *28*, 4314−4318.
(8) Hamza, M. S. A.; Zou, X.; Brown, K. L.; van Eldik, R. *Inorg. Chem.* **2001**, *40*, 5440−5447.
(9) Brown, K. L.; Cheng, S.; Zou, X.; Zubkowski, J. D.; Valente, E. J.; Knapton, L.; Marques, H. M. *Inorg. Chem.* **1997**, *36*, 3666−3675.
(10) Knapton, L.; Marques, H. M. *Dalton Trans.* **2005**, 889−895.
(11) Perry, C. B.; Fernandes, M. A.; Brown, K. L.; Zou, X.; Valente, E. J.; Marques, H. M. *Eur. J. Inorg. Chem.* **2003**, 2095−2107.
(12) Chemaly, S. M.; Brown, K. L.; Fernandes, M. A.; Munro, O. Q.; Grimmer, C.; Marques, H. M. *Inorg. Chem.* **2011**, *50*, 8700−8718.
(13) Perry, C. B.; Marques, H. M. *S. Afr. J. Chem.* **2005**, *58*, 9−15.
(14) Navizet, I.; Perry, C. B.; Govender, P. P.; Marques, H. M. *J. Phys. Chem. B* **2012**, *116*, 8836−8846.
(15) Govender, P. P.; Navizet, I.; Perry, C. B.; Marques, H. M. *Chem. Phys. Lett.* **2012**, *550*, 150−155.
(16) Marques, H. M.; Knapton, L. *J. Chem. Soc., Dalton Trans.* **1997**, 3827−3833.
(17) Marques, H. M.; Knapton, L.; Zou, X.; Brown, K. L. *J. Chem. Soc., Dalton Trans.* **2002**, 3195−3200.
(18) Chemaly, S. M.; Florczak, M.; Dirr, H.; Marques, H. M. *Inorg. Chem.* **2011**, *50*, 8719−8727.
(19) Chemaly, S. M.; Kendall, L.; Nowakowska, M.; Pon, D.; Perry, C. B.; Marques, H. M. *Inorg. Chem.* **2013**, *52*, 1077−1083.
(20) Garau, G.; Geremia, S.; Marzilli, L. G.; Nardin, G.; Randaccio, L.; Tauzher, G. *Acta Crystallogr., Sect. B* **2003**, 51−59.
(21) Gross, Z. *J. Biol. Inorg. Chem.* **2001**, *6*, 733−738.
(22) Gryko, D. T. *Eur. J. Org. Chem.* **2002**, 1735−1743.
(23) Mathura, S.; Sannasy, D.; de Sousa, A. S.; Perry, C. B.; Navizet, I.; Marques, H. M. *J. Inorg. Biochem.* **2013**, *123*, 66−79.
(24) Aviv-Harel, I.; Gross, Z. *Chem.—Eur. J.* **2009**, *15*, 8382−8394.
(25) Joseph, C. A.; Ford, P. C. *J. Am. Chem. Soc.* **2005**, *127*, 6737−6743.
(26) Paolesse, R.; Jaquinod, L.; Nurco, D. J.; Mini, S.; Sagone, F.; Boschi, T.; Smith, K. M. *Chem. Commun.* **1999**, 1307−1308.
(27) Gross, Z.; Galili, N.; Saltsman, I. *Angew. Chem., Int. Ed.* **1999**, *38*, 1427−1429.
(28) Koszarna, B.; Gryko, D. T. *J. Org. Chem.* **2006**, *71*, 3707−3717.
(29) Paolesse, R.; Nardis, S.; Sagone, F.; Khoury, R. G. *J. Org. Chem.* **2001**, *66*, 550−556.
(30) Gross, Z.; Galili, N.; Simkhovich, L.; Saltsman, I.; Botoshansky, M.; Blaser, D.; Boese, R.; Goldberg, I. *Org. Lett.* **1999**, *1*, 599−602.
(31) Gryko, D. T.; Jadach, K. *J. Org. Chem.* **2001**, *66*, 4267−4275.
(32) Roa, P. D.; Dhanalekshmi, S.; Little, B. J.; Lindsey, J. S. *J. Org. Chem.* **2000**, *65*, 7323−7344.
(33) Lee, C.-H.; Lindsey, J. S. *Tetrahedron* **1994**, *50*, 11427−11440.
(34) Decréau, R. A.; Collman, J. P. *Tetrahedron Lett.* **2003**, *44*, 3323−3327.
(35) Itahara, T. *J. Chem. Soc., Chem. Commun.* **1980**, 49−50.
(36) Fu, L.; Gribble, G. W. *Tetrahedron Lett.* **2008**, *49*, 7352−7354.
(37) Erben, C.; Will, S.; Kadish, K. M. In *The Porphyrin Handbook;* Kadish, K. M., Smith, K. M., Guilard, R., Eds.; Academic Press: New York, 2000; Vol. 2, pp 233−300.
(38) Mahammed, A.; Gray, H. B.; Weaver, J. J.; Sorasaenee, K.; Gross, Z. *Bioconjugate Chem.* **2004**, *15*, 738−746.
(39) Zipp, C. F.; Michael, J. P.; Fernandes, M. A.; Marques, H. M. *S. Afr. J. Chem.* **2013**, *66*, 158−166.
(40) Young, R.; Chang, C. K. *J. Am. Chem. Soc.* **1985**, *107*, 898−909.
(41) Liu, J.-G.; Naruta, Y.; Tani, F. *Angew. Chem., Int. Ed.* **2005**, *44*, 1836−1840.
(42) Collman, J. P.; Decréau, R. A. *J. Org. Chem.* **2004**, *69*, 3546−3549.
(43) Liu, J.-G.; Ohta, T.; Yamaguchi, S.; Ogura, T.; Sakamoto, S.; Maeda, Y.; Naruta, Y. *Angew. Chem., Int. Ed.* **2009**, *48*, 9262−9267.
(44) Berto, T. C.; Praneeth, V. K. K.; Goodrich, L. E.; Lehnert, N. *J. Am. Chem. Soc.* **2009**, *131*, 17116−17126.
(45) Karlin, K. D. *Nature* **2010**, *463*, 168−169.
(46) Decréau, R. A.; Collman, J. P.; Yang, Y.; Yan, Y.; Devaraj, N. K. *J. Org. Chem.* **2007**, *72*, 2794−2802.
(47) Didier, A.; Michaudet, L.; Ricard, D.; Baveux-Chambenoît, V.; Richard, P.; Boitrel, B. *Eur. J. Org. Chem.* **2001**, 1917−1926.
(48) Collman, J. P.; Sunderland, C. J.; Boulatov, R. *Inorg. Chem.* **2002**, *41*, 2282−2291.
(49) Collman, J. P.; Decréau, R. A. *Org. Lett.* **2005**, *7*, 975−978.
(50) Collman, J. P.; Bröring, M.; Fu, L.; Rapta, M.; Schwenninger, R. *J. Org. Chem.* **1998**, *63*, 8084−8085.
(51) Zipp, C. F.; Dirr, H. W.; Fernandes, M. A.; Marques, H. M.; Michael, J. P. *Cryst. Growth Des.* **2013**, *13*, 3463−3474.
(52) White, W. I. In *The Porphyrins;* Dolphin, D., Ed.; Academic Press: New York, 1978; Vol. *V*.
(53) Pasternack, R. F.; Huber, P. R.; Boyd, P.; Engasser, G.; Francesconi, L.; Gibbs, E.; Fasella, P.; Venturo, G. C.; de Hinds, L. C. *J. Am. Chem. Soc.* **1972**, *94*, 4511−4517.
(54) Aron, J.; Baldwin, D. A.; Marques, H. M.; Pratt, J. M.; Adams, P. A. *J. Inorg. Biochem.* **1986**, *27*, 227−243.
(55) Munro, O. Q.; Marques, H. M. *Inorg. Chem.* **1996**, *35*, 3752−3767.
(56) Betterton, E. A. Ph.D. Thesis, University of the Witwatersrand: Johannesburg, 1982.
(57) Hanania, G. I. H.; Irvine, D. H. *J. Chem. Soc.* **1964**, 5694−5697.
(58) Randall, W. C.; Alberty, R. A. *Biochemistry* **1967**, *6*, 1520−1525.
(59) Rubinson, K. A.; Parekh, H. V.; Mark, H. B. *Inorg. Chem.* **1983**, *22*, 458−463.
(60) Hayward, G. C.; Hill, H. A. O.; Pratt, J. M.; Vanston, N. J.; Williams, R. J. P. *J. Chem. Soc. A* **1965**, 6485−6493.
(61) Smith, E. L.; Fantes, K. H.; Ball, S.; Waller, J. G.; Emery, W. B.; Anslow, W. K.; Walker, A. D. *Biochem. J.* **1952**, *52*, 389−395.
(62) Fantes, K. H.; Page, J. E.; Parker, L. F. J.; Smith, E. L. *Proc. R. Soc. B* **1950**, *136*, 592−609.
(63) Prinsloo, F. F.; Breet, E. L. J.; van Eldik, R. *J. Chem. Soc., Dalton Trans.* **1995**, 685−688.
(64) Pratt, J. M. *The Inorganic Chemistry of Vitamin B_{12};* Academic Press: London, 1972.
(65) Reichardt, C.; Welton, T. *Solvents and Solvent Effects in Organic Chemistry,* 4th ed.; Wiley Verlag Chemie: Weinheim, Germany, 2011.
(66) Smithrud, D. B.; Sanford, E. M.; Chao, I.; Ferguson, S. B.; Carcanague, D. R.; Evanseck, J. D.; Houk, K. N.; Diederich, F. *Pure Appl. Chem.* **1990**, *62*, 2227−2236.
(67) Hamza, M. S. A. *J. Inorg. Biochem.* **1998**, *69*, 269−274.
(68) Mathura, S. PhD Thesis, University of the Witwatersrand: 2013.
(69) Firth, R. A.; Hill, H. A. O.; Pratt, J. M.; Thorp, R. G.; Williams, R. J. P. *J. Chem. Soc. A* **1969**, 381−386.
(70) Chemaly, S. M. *J. Inorg. Biochem.* **1991**, *44*, 17−25.
(71) Hill, H. A. O.; Pratt, J. M.; Thorp, R. G.; Ward, B.; Williams, R. J. P. *Biochem. J.* **1970**, *120*, 263−269.
(72) Moreno-Esparza, R.; Lopez, M.; Peannell, K. H. *J. Chem. Soc., Dalton Trans.* **1992**, 1791−1795.
(73) Bader, R. F. W.; Matta, C. F.; Cortés-Guzmán, F. *Organometallics* **2004**, *23*, 6253−6263.
(74) Espinosa, E.; Souhassou, M.; Lachekar, H.; Lecomte, C. *Acta Crystallogr., Sect. B* **1999**, *55*, 563−572.
(75) Howard, S. T.; Krygowski, T. M. *Can. J. Chem.* **1997**, *75*, 1174−1181.
(76) Grabowski, S. J. *J. Phys. Chem. A* **2000**, *105*, 5551−5557.
(77) Vidal, I.; Melchor, S.; Alkorta, I.; Elguero, J.; Sundberg, M. R.; Dobado, J. A. *Organometallics* **2006**, *25*, 5638−5647.
(78) Espinosa, E.; Alkorta, I.; Elguero, J.; Molins, E. *J. Chem. Phys.* **2002**, *117*, 5529−5542.
(79) Balt, S.; de Bolster, M. W. G.; van Herk, A. M. *Inorg. Chim. Acta* **1985**, *107*, 13−17.
(80) Bader, R. F. *Atoms in Molecules: A Quantum Theory;* Oxford University Press: Oxford, U.K., 1990.
(81) Varadwaj, P. R.; Cukrowski, I.; Marques, H. M. *J. Phys. Chem. A* **2008**, *112*, 10657−10666.
(82) Varadwaj, P. R.; Cukrowski, I.; Perry, C. B.; Marques, H. M. *J. Phys. Chem. A* **2011**, *115*, 6629−6640.
(83) Varadwaj, P. R.; Marques, H. M. *Phys. Chem. Chem. Phys.* **2010**, *12*, 2126−2138.

(84) Varadwaj, P. R.; Marques, H. M. *Theor. Chem. Acc.* **2010**, *127*, 711−725.
(85) Varadwaj, P. R.; Varadwaj, A.; Marques, H. M. *J. Phys. Chem. A* **2011**, *115*, 5592−5601.
(86) Varadwaj, P. R.; Varadwaj, A.; Peslherbe, G. H.; Marques, H. M. *J. Phys. Chem. A* **2011**, *115*, 13180−13190.
(87) *Systat Software,* 11.0.0.75; SigmaPlot: San Jose, CA, 2008.
(88) *MestReNova,* v. 6.0.2−5475; Mestrelab Research : Santiago de Compostela, Spain, 2009.
(89) Hill, J. A.; Pratt, J. M.; Williams, R. J. P. *J. Chem. Soc. A* **1964**, 5149−5153.
(90) PG Instruments, Leicestershire, UK, 2012.
(91) Kirino, O.; Yamamoto, S.; Kato, T. *Agric. Biol. Chem.* **1980**, *44*, 2143−2147.
(92) Marques, H. M.; Munro, O. Q.; Crawcour, M. L. *Inorg. Chim. Acta* **1992**, *196*, 221−229.
(93) Conn, J. B.; Wartman, T. G. *Science* **1952**, *115*, 72−73.
(94) Marques, H. M.; Brown, K. L.; Jacobsen, D. W. *J. Biol. Chem.* **1988**, *263*, 12378−12383.
(95) Wang, J.; Wolf, R.; Caldwell, J. W.; Kollman, P. A.; Case, D. A. *J. Comput. Chem.* **2004**, *25*, 1157−1174.
(96) Hypercube, Inc.: 7.03, Gainesville, FL, 2002.
(97) Marques, H. M.; Ngoma, B.; Egan, T. J.; Brown, K. L. *J. Mol. Struct.* **2001**, *561*, 71−91.
(98) Allen, F. H. *Acta Crystallogr., Sect. B* **2002**, *B58*, 380−388.
(99) Bruno, I. J.; Cole, J. C.; Edgington, P. R.; Kessler, M.; Macrae, C. F.; McCabe, P.; Pearson, J.; Taylor, R. *Acta Crystallogr.* **2002**, *B58*, 389−397.
(100) Anderson, W. P.; Edwards, W. D.; Zerner, M. C. *Inorg. Chem.* **1986**, *25*, 2728−2732.
(101) *Gaussian 09,* Revision A.02; Gaussian, Inc: Wallingford, CT, 2009.
(102) Becke, A. D. *Phys. Rev. A* **1988**, *38*, 3098−3100.
(103) Perdew, J. P.; Wang, Y. *Phys. Rev. B* **1986**, *33*, 8822−8824.
(104) Schäfer, A.; Horn, H.; Ahlrichs, R. *J. Chem. Phys.* **1992**, *97*, 2571−2577.
(105) Schäfer, A.; Huber, C.; Ahlrichs, R. *J. Chem. Phys.* **1994**, *100*, 5829−5835.
(106) Dunlap, B. I. *J. Chem. Phys.* **1983**, *78*, 3140−3142.
(107) Dunlap, B. I. *J. Mol. Struct.: THEOCHEM* **2000**, *529*, 37−40.
(108) Eichkorn, K.; Treutler, O.; Öhm, H.; Häser, M.; Ahlrichs, R. *Chem. Phys. Lett.* **1995**, *240*, 283−290.
(109) Eichkorn, K.; Weigend, F.; Treutler, O.; Ahlrichs, R. *Theor. Chem. Acc.* **1997**, *97*, 119−124.
(110) Yanai, T.; Tew, D. P.; Handy, N. C. *Chem. Phys. Lett.* **2004**, *393*, 51−57.
(111) *AIMAll* (Version 11.12.19), http://aim.tkgristmill.com, 08.05.04, Overland Park, KS, 2011.